Electronic Supplementary Material (ESI) for Dalton Transactions

Supramolecular lanthanide metallogrids exhibiting field-induced single-ion magnetic behavior

Shu-Qi Wu,[†] Qi-Wei Xie,[†] Guang-Yu An,[†] Xi-Chen,[†] Cai-Ming Liu,[‡] Ai-Li Cui,[†] Hui-Zhong Kou[†]*

[†]Department of Chemistry, Tsinghua University, Beijing 300071, P. R. China. Email: kouhz@mail.tsinghua.edu.cn

[‡]Beijing National Laboratory for Molecular Sciences, Center for Molecular Science, Institute of Chemistry, Chinese Academy of Sciences, Beijing 100190, P. R. China.

Experimental details

Physical Measurements

IR spectra were recorded on a Nicolet Magna-IR 750 spectrometer in the 4000-650 cm^{-1} region. Elemental analyses (C, H, N) were performed on an Elementar Vario MICRO CUBE analyzer. ESI-MS spectra were performed on ThermoFisher LTQ Orbitrap XL. Temperature- and field-dependent magnetic susceptibility measurements were carried out on a Quantum Design SQUID magnetometer. Well-shaped single crystals were collected and used for magnetic measurements. The experimental susceptibilities were corrected for the diamagnetism of the constituent atoms (Pascal's Tables).

Single crystal X-ray data were collected on a Rigaku Saturn724+ CCD diffractometer at 153 K for complex **1** and at 143 K for complex **2**. The structures were solved by direct method (SHELXS-97) and refined by full-matrix least-squares (SHELXL-97) on F^2. Anisotropic thermal parameters were used for the non-hydrogen atoms and isotropic parameters for the hydrogen atoms. Hydrogen atoms were added geometrically and refined using a riding model. There presents site disorder in one pyridine group of the ligand H_2L^{2-} in complex **2**, and occupancies have been set as 0.6:0.4 during the structural refinement. Due to the weak diffraction and/or disordered solvents, the methanol and the azide anions cannot be completely modeled. The SQUEEZE function of PLATON was applied, and gave available voids of 3299.3 $Å^3$ and 3516.3 $Å^3$ for complex **1** and **2,** respectively. The corresponding residual electron counts were 724 e^- and 575 e^- per unit cell, corresponding to the missing solvent molecules.

Synthesis of 4,6-dihydroxy-5-methylisophthalaldehyde

Hexamethylenetetramine (14.00 g, 100 mmol) and 2-methylbenzene-1,3-diol (6.20 g, 50 mmol) was added to 100 mL trifluoroacetic acid under N_2 atmosphere. The solution was heated to 100°C for 3 h. Then 150 mL of 3 M HCl was added, and the solution was heated at 100°C for 4 h. After cooling to room temperature, the solution was filtered through Celite. The precipitate was collected and dried under vacuum.

4.22 g of white powder (23 mmol, 46%) was afforded.

Synthesis of H_4L

4,6-dihydroxy-5-methylisophthalaldehyde (1.80 g, 10 mmol) was suspended in 40 mL methanol, and then solid isonicotinyl hydrazide (2.74 g, 20 mmol) was slowly added in. The mixture was dissolved when refluxed, and gradually precipitated. The solution was filtered through Celite. The precipitate was collected and dried under vacuum. 3.80 g of pale yellow powder (9.0 mmol, 90%) was afforded. M.P.: >300°C, decompose.

Synthesis of complexes 1 and 2

Reaction of H_4L with $LnCl_3 \cdot 6H_2O$ (Ln^{III} = Dy^{III}, Tb^{III}) in methanol gave a crimson solution. As 8 equiv of solid NaN_3 was added to the above solution, orange precipitate formed immediately. DMF was slowly added dropwise until the turbid solution became limpid again. Slow evaporation of the DMF-MeOH solution gave the orange single crystals of complexes **1** and **2** in yield of about 20%. Elemental analyses (%): calcd for $C_{104}H_{141}Dy_4N_{35}O_{37}Cl_2$ (complex **1**): C 39.10, H 4.45, N 15.35; Found: C 39.53, H 4.79, N 15.35. Calcd for $C_{106}H_{149}Tb_4N_{35}O_{39}Cl_2$ (complex **2**): C 39.24, H 4.63, N 15.11; Found: C 39.79, H 4.85, N 15.20.

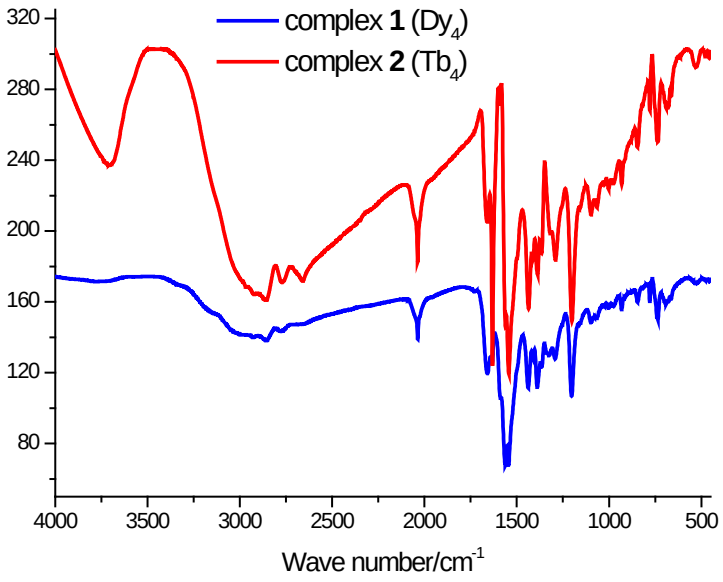

Figure S1. IR spectra of complexes **1** and **2** in KBr pellets.

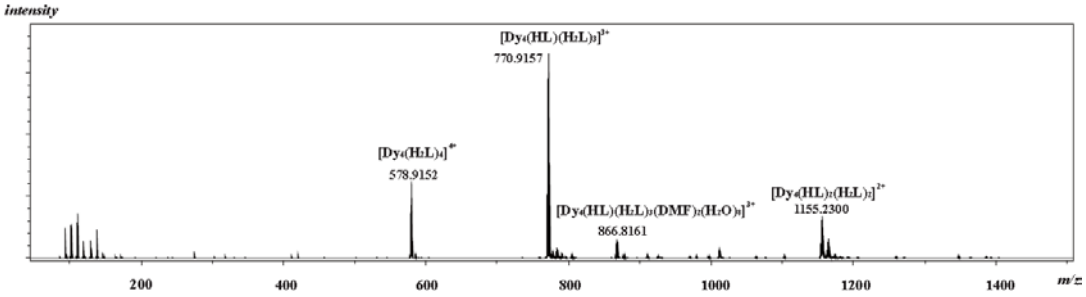

Figure S2. ESI-MS Spectroscopy of complex **1** in DMF.

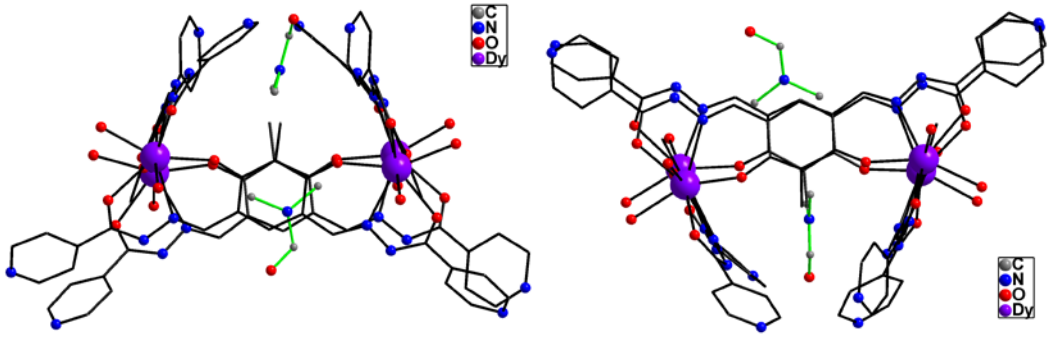

Figure S3. Guest DMF molecules in the cavity of the metallogrid (complex **1**).

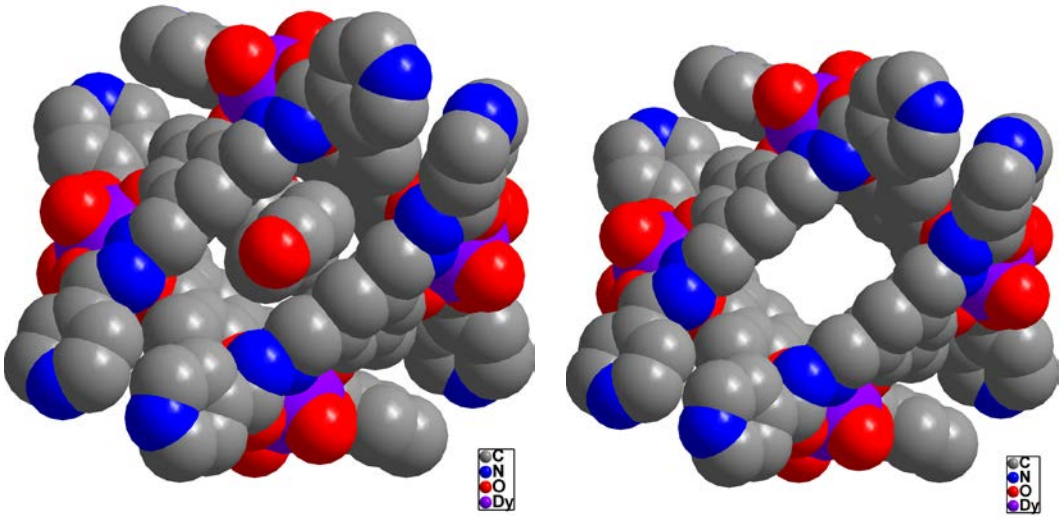

Figure S4. Space-filling diagram of complex **1** showing the cavity of the grid molecule. Right: Encapsulated DMF molecules are shown. Left: The DMF molecules are removed.

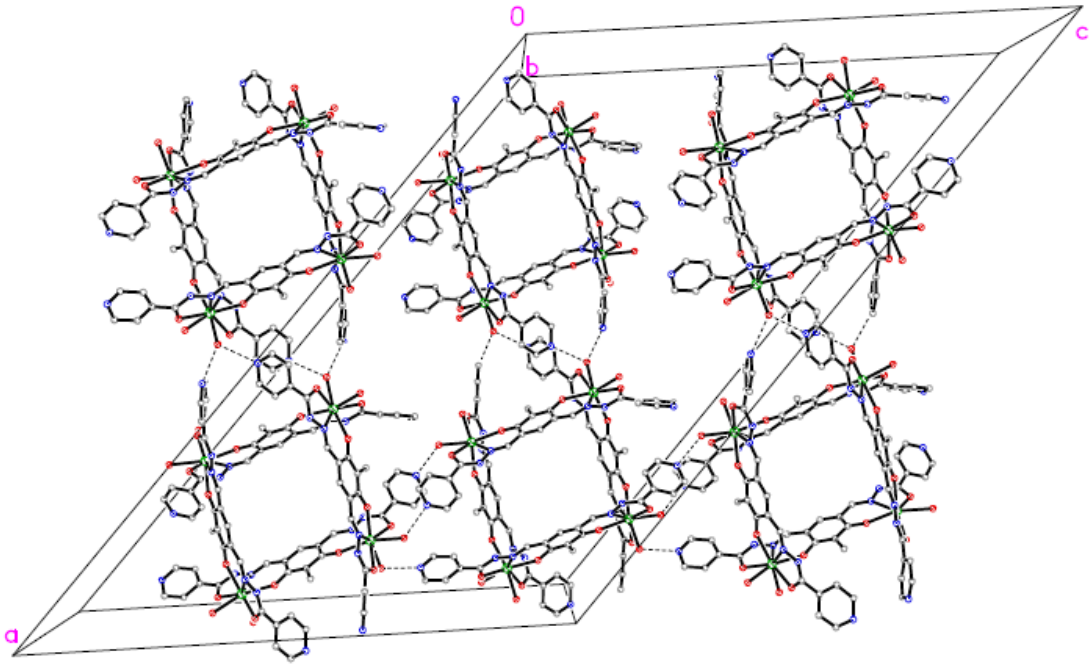

Figure S5. Hydrogen bonding interactions (dotted lines) in complex **1**.

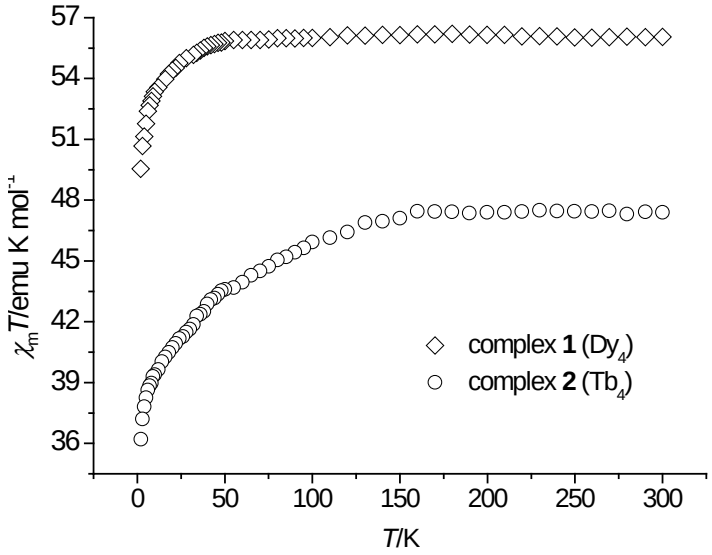

Figure S6. Temperature dependence of $\chi_m T$ for complexes **1** and **2**.

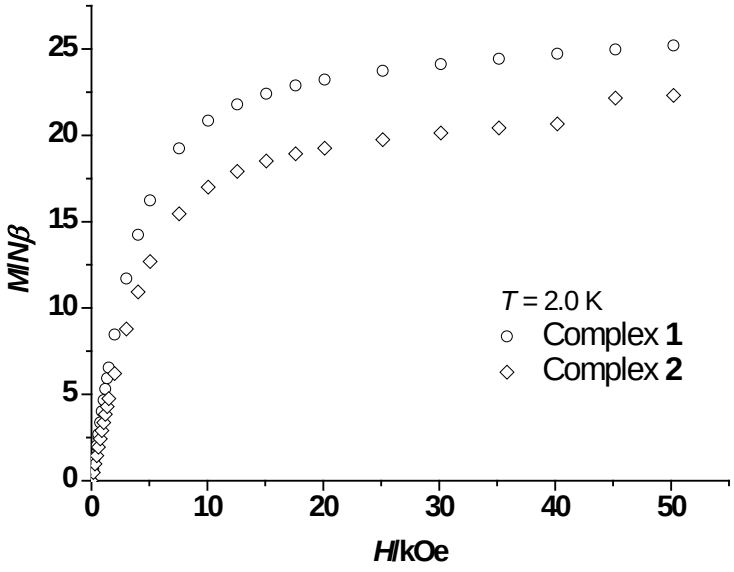

Figure S7. Field dependence of magnetization for complex **1** and **2** at 2.0 K.

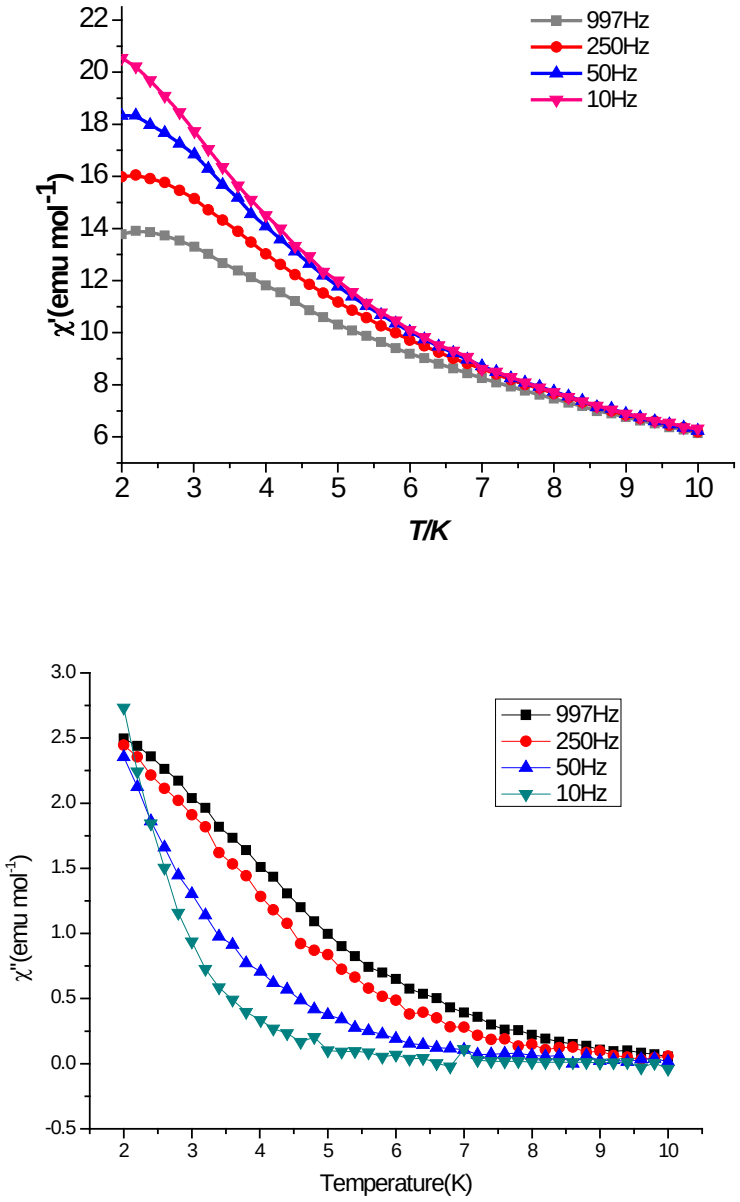

Figure S8. Temperature dependence of in-phase (top) and out-of-phase (bottom) susceptibility of complex **1** under 1 kOe dc field.

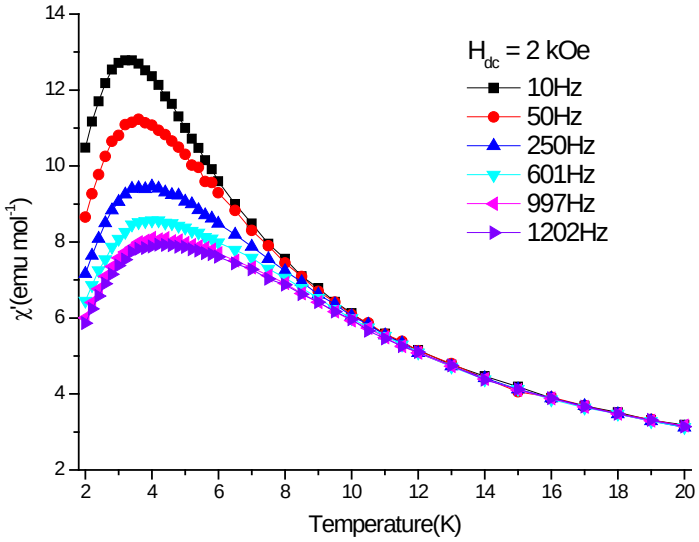

Figure S9. Temperature dependence of in-phase susceptibility of complex **1** under 2 kOe dc field.

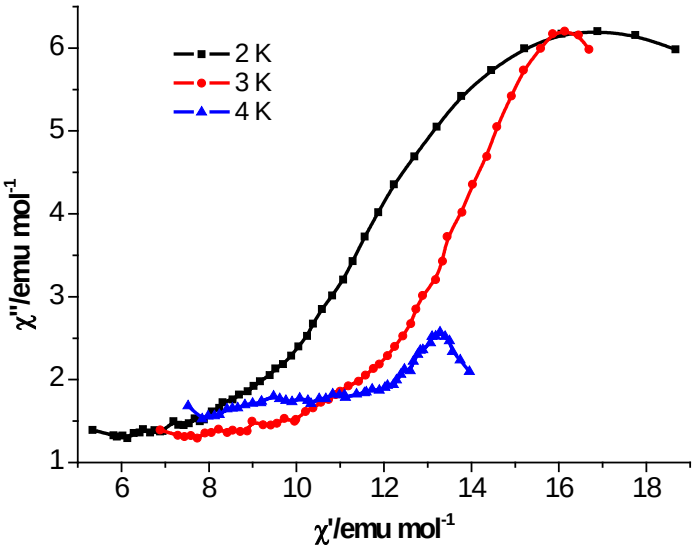

Figure S10. Cole-Cole curves of complex **1** under 2 kOe below 4 K.

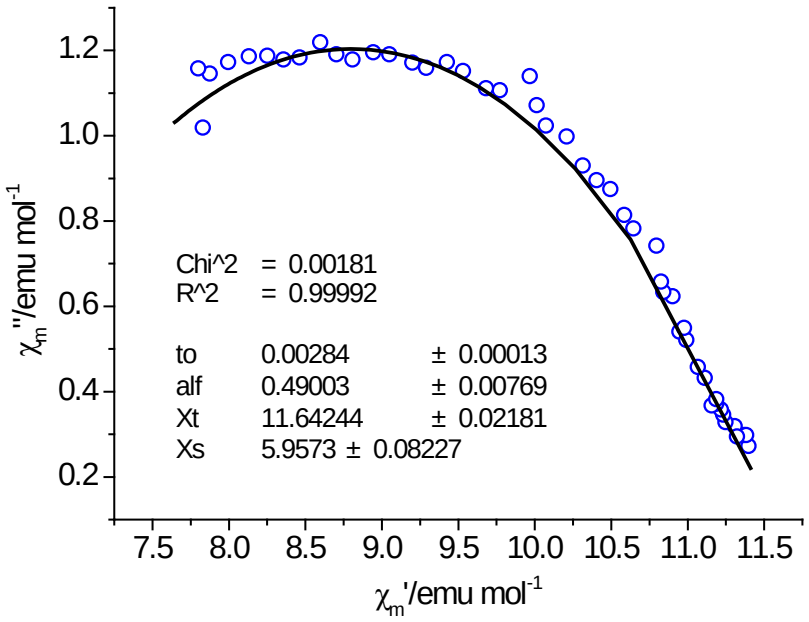

Figure S11. Cole-Cole curves of complex **1** under 2 kOe at 5 K. The solid line represents the fit using the modified Debye equation.

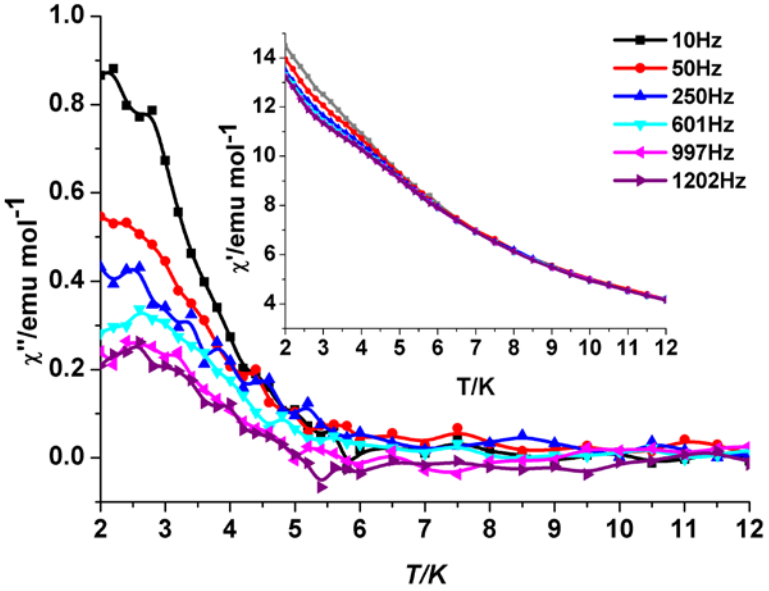

Figure S12. Temperature dependence of out-of-phase susceptibility (χ_m'') of complex **2** at different frequencies under a 2 kOe dc field. Insert: Temperature dependence of in-phase susceptibility (χ_m') of complex **2**.

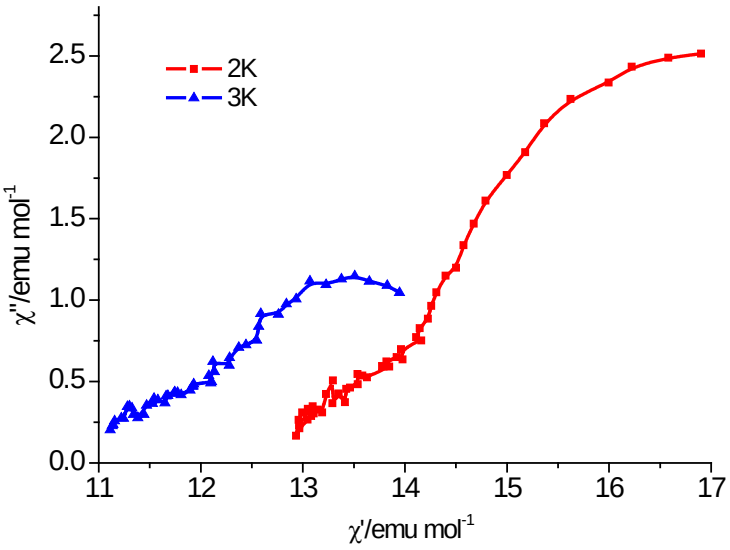

Figure S13. Cole-Cole curves of complex **2** under 2 kOe at various temperatures.